Nanobody derived using a peptide epitope from the spike protein receptor-binding motif inhibits entry of SARS-CoV-2 variants

Nivya Mendon[1,2,‡], **Rayees A. Ganie**[1,2,‡], **Shubham Kesarwani**[1,‡], **Drisya Dileep**[1,3] , **Sarika Sasi**[1], **Prakash Lama**[1,2], **Anchal Chandra**[4] , and **Minhajuddin Sirajuddin**[1,*]

From the [1]Centre for Cardiovascular Biology and Disease, Institute for Stem Cell Science and Regenerative Medicine, GKVK Campus, Bengaluru, India; [2]Manipal Academy of Higher Education, Manipal, Karnataka, India; [3]The University of Trans-Disciplinary Health Sciences and Technology (TDU), Bengaluru, India; [4]National Centre for Biological Sciences, TIFR, GKVK Campus, Bengaluru, India

Edited by Dennis Voelker

The emergence of new escape mutants of the severe acute respiratory syndrome coronavirus 2 (SARS-CoV-2) has escalated its penetration among the human population and has reinstated its status as a global pandemic. Therefore, developing effective antiviral therapy against emerging SARS-CoV variants and other viruses in a short period becomes essential. Blocking SARS-CoV-2 entry into human host cells by disrupting the spike glycoprotein-angiotensin-converting enzyme 2 interaction has already been exploited for vaccine development and monoclonal antibody therapy. Unlike the previous reports, our study used a nine-amino acid peptide from the receptor-binding motif of the spike protein as an epitope. We report the identification of an efficacious nanobody N1.2 that blocks the entry of pseudovirus-containing SARS-CoV-2 spike as the surface glycoprotein. Moreover, using mCherry fluorescence-based reporter assay, we observe a more potent neutralizing effect against both the hCoV19 (Wuhan/WIV04/2019) and the Omicron (BA.1) pseudotyped spike virus with a bivalent version of the N1.2 nanobody. In summary, our study presents a rapid and efficient methodology to use peptide sequences from a protein–receptor interaction interface as epitopes for screening nanobodies against potential pathogenic targets. We propose that this approach can also be widely extended to target other viruses and pathogens in the future.

The severe acute respiratory syndrome coronavirus 2 (SARS-CoV-2) belongs to the betacoronavirus family and is the third member of the family after Middle East respiratory syndrome coronavirus and SARS-CoV that has infected the human population, resulting in moderate to severe pathogenic symptoms (1). With the frequent outbreaks of new variants, these numbers are increasing every day (2). Although several safe and effective anti-SARS-CoV-2 therapies exist, which can prevent severe symptoms upon infection, none of them has been proven to be 100% effective. Partial vaccination, in turn, has put the SARS-CoV-2 virus under increased selection pressure resulting in a high mutation rate in the viral spike protein (3). With the emergence of novel variants and escape mutants of SARS-CoV-2, there is an urgent need to develop effective antiviral therapy that can function as a panacea for both the current and emerging variants.

The surface of the SARS-CoV-2 virus is decorated with homotrimer spike envelope glycoprotein, the major antigenic determinant of the host immune response and one of the main coronavirus drug targets (4). The SARS-CoV-2 entry is orchestrated by the interaction of the receptor-binding domain (RBD) of its spike with the angiotensin-converting enzyme 2 (ACE2) receptor on the host cell membrane (5, 6). The interaction is established by a set of conserved residues present in the receptor-binding motif (RBM) of the spike (7). Efforts have been made to prevent this first step of infection using antibodies or nanobodies that target the spike–ACE2 interaction (8–17). Several groups have also isolated antibodies directly from convalescent SARS-CoV-2 patients that showed promising neutralization against SARS-CoV-2 *in vitro* and improved clinical outcomes in tested animals *in vivo* (18–23). Nanobodies, on the other hand, offer many advantages over conventional antibodies in terms of their size, high thermal stability, solubility, and ease of expression in bacteria, hence making them easily scalable and cost-effective therapies (24). Nanobodies, which are derived from the variable domain of the camelid heavy chain, retain specificity and affinity similar to conventional antibodies. Modularity in nanobodies allows oligomerization, hence increasing their avidity and serum shelf life (25). Nanobodies can be easily humanized, which is critical for developing antiviral therapies for humans (26). Treatment with combinatorial nanobodies has been effective in neutralizing SARS-CoV-2 and preventing mutational escape (11). Many of such anti-SARS-CoV-2 therapies report the use of the entire spike protein or its RBD as the epitope to screen active antiviral antibodies (8–17). A limitation of using the entire spike protein or RBD as an epitope is that the isolated antibodies may bind to different regions of spike protein other

---

‡ These authors contributed equally to this work.
* For correspondence: Minhajuddin Sirajuddin, minhaj@instem.res.in.

than the ACE2-interacting domain, thus rendering them unspecific and inefficient in fully neutralizing the viral infection. Here, we report the isolation of a nanobody (N1.2) from a yeast nanobody display library using a nine-amino acid peptide sequence as a target epitope. The peptide was designed from the specific residues present in the RBM of spike protein showing maximum interaction with the ACE2 receptor. This nanobody, both the monomer as well as the tandem dimer, interferes with ACE2 binding, thus showing a potent virus neutralization activity in cellular models.

Results

Screening and identification of antispike nanobodies

SARS-CoV-2 interacts with the cellular ACE2 receptor in the host cell plasma membrane *via* its trimeric spike envelope protein to gain access to the cytoplasm (Fig. 1A). We designed two peptide sequences from the spike envelope protein; peptide-1 (residues 486–494) and peptide-2 (residues 496–505) from the RBM of hCoV19 (Wuhan/WIV04/2019) (5). The choice of these two peptides was based on contact site and strength of interaction of RBD with ACE2. The 19-residue RBM stretch encompassing both the peptides has the maximum interaction sites with ACE2, which involves nine hydrogen bonds (5). In addition, the RBM stretch is devoid of glycosylation sites reported so far in the analysis of SARS-CoV-2 spike protein (27), thus making the peptides an ideal candidate for nanobody screening. These peptides were used as bait (epitope) to enrich potential nanobody sequences from the combinatorial yeast display library (28). The screening methodology involves two rounds of magnetic screening followed by fluorescent-activated cell sorting (FACS)–based enrichment of the library (Fig. 1B). From the FACS analysis, only peptide-1 showed positive enrichment of the nanobody clones (Fig. 1B). Therefore, from here onward, we focused only on the nanobody population obtained from the peptide-1 screen. After FACS, the enriched yeast clones were individually analyzed using sequencing. Ten unique nanobody sequences were identified and purified, named N1.1 to N1.10, for further characterization (Fig. S1 and Table S1) (see the Experimental procedures section).

These purified nanobodies were subjected to ELISA for characterizing the interaction with peptide-1 and peptide-2 (see the Experimental procedures section). All the nanobodies showed binding with the peptide-1 compared with the peptide-2, except N1.4 (Fig. 1C), suggesting that the enriched nanobody clones N1.1 to N1.10 are specific toward the peptide-1 epitope.
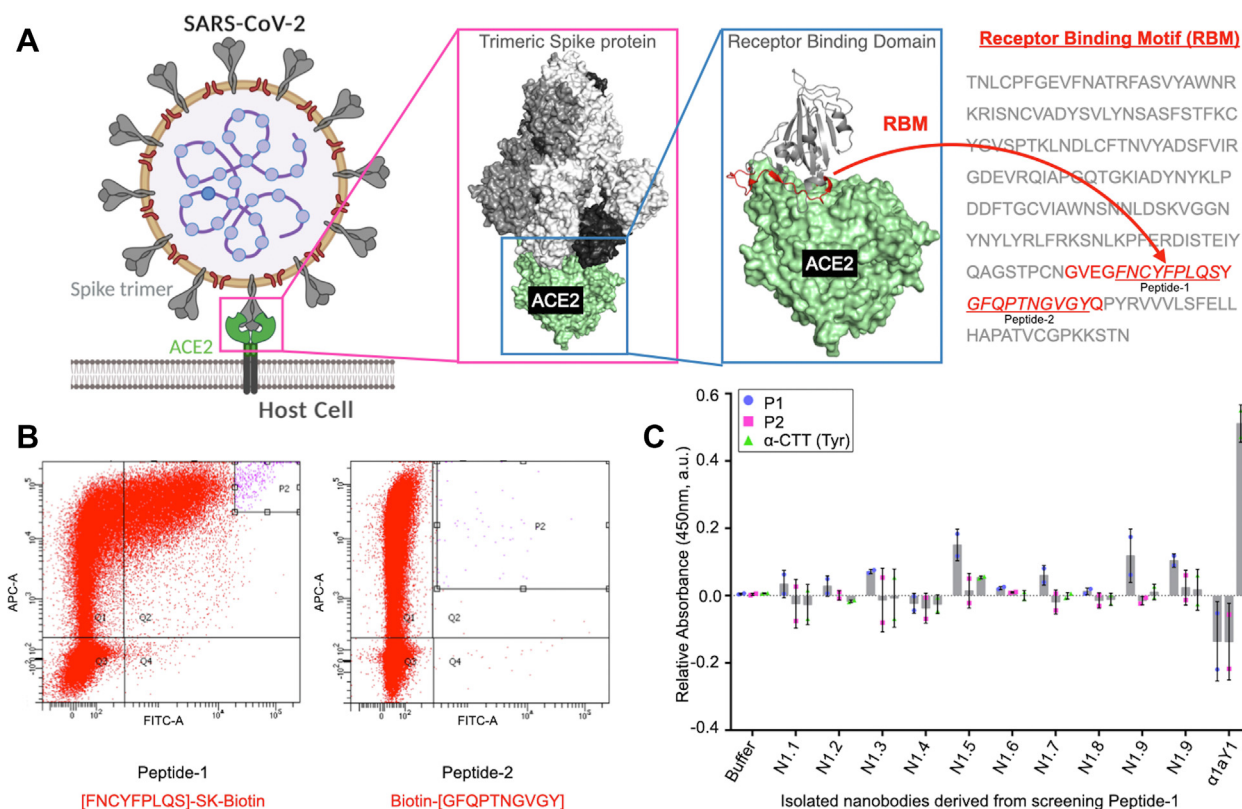

Figure 1. Identification of nanobodies against spike protein using peptides. *A,* schematic illustration of SARS-CoV-2 virus entry into the host cell through ACE2 receptor. *Cartoon* model of molecular interaction between spike- and RBD-ACE2 derived from Protein Data Bank (codes: 6VXX and 6LZG, respectively). The receptor binding motif (RBM) is highlighted in *red* in the *ribbon* model and sequence, and the peptide-1 and peptide-2 sequences are underscored and indicated. *B,* representative images for peptide-1 and peptide-2 sorting data on BD FACS Aria fusion cell sorter, the nanobody library labeled using anti-HA marker in Alexa Fluor-647 channel, and the peptides with streptavidin FITC. The P2 quadrant represents the double labeled yeast population indicating the extent of enrichment of yeast clones that has an affinity toward the respective peptide. *C,* ELISA of purified nanobodies against the peptide-1, peptide-2, and tyrosinated alpha-tubulin CTT peptide are shown as scatter plots with average values as *column bar* with error bar representing standard deviation. N = 2. The A1aY1 protein against tyrosinated alpha-tubulin CTT peptide was included as an assay control. ACE2, angiotensin-converting enzyme 2; CTT, carboxy terminal tail; HA, hemagglutinin; RBD, receptor-binding domain; SARS-CoV-2, severe acute respiratory syndrome coronavirus 2.

Characterization of nanobodies using flow cytometry–based cellular assay

We then tested each of the purified nanobodies for their ability to block spike–ACE2 interaction using a pseudovirus-based neutralizing assay (Fig. 2A). Pseudoviruses displaying spike envelope glycoprotein with a mCherry reporter were generated (29) (see the Experimental procedures section). The viral infectivity was assessed using the mCherry expression, which was further quantified using fluorescence measurement (see the Experimental procedures section).

Since the ACE2 expression in human embryonic kidney 293T (HEK293T) cells is lower compared with other cell lines (30, 31), we generated an ACE2-expressing stable HEK293T cell line, herein referred to as enhanced GFP (eGFP)-ACE2/HEK293T cells (see the Experimental procedures section). The

eGFP-ACE2/HEK293T stable cell lines also coexpressed eGFP as a fluorescent marker to facilitate identifying the ACE2-expressing cells (Figs. 2B and S2) (see the Experimental procedures section). The eGFP-ACE2/HEK293T cells were transduced with varying dilutions of spike pseudoviruses (see the Experimental procedures section). Quantification using FACS analysis showed ~75%, 55%, 16%, and 4% of cells transduced with mCherry fluorescence correlating with the varying dilution of pseudoviruses, respectively (Fig. S3, A and B). We characterized the transduction efficiency of the pseudovirus as a function of its multiplicity of infection (MOI). To test the efficacy of nanobodies in blocking viral entry, we choose to perform experiments with pseudovirus MOI that yield >70% transduction efficiency and low cellular cytotoxicity.
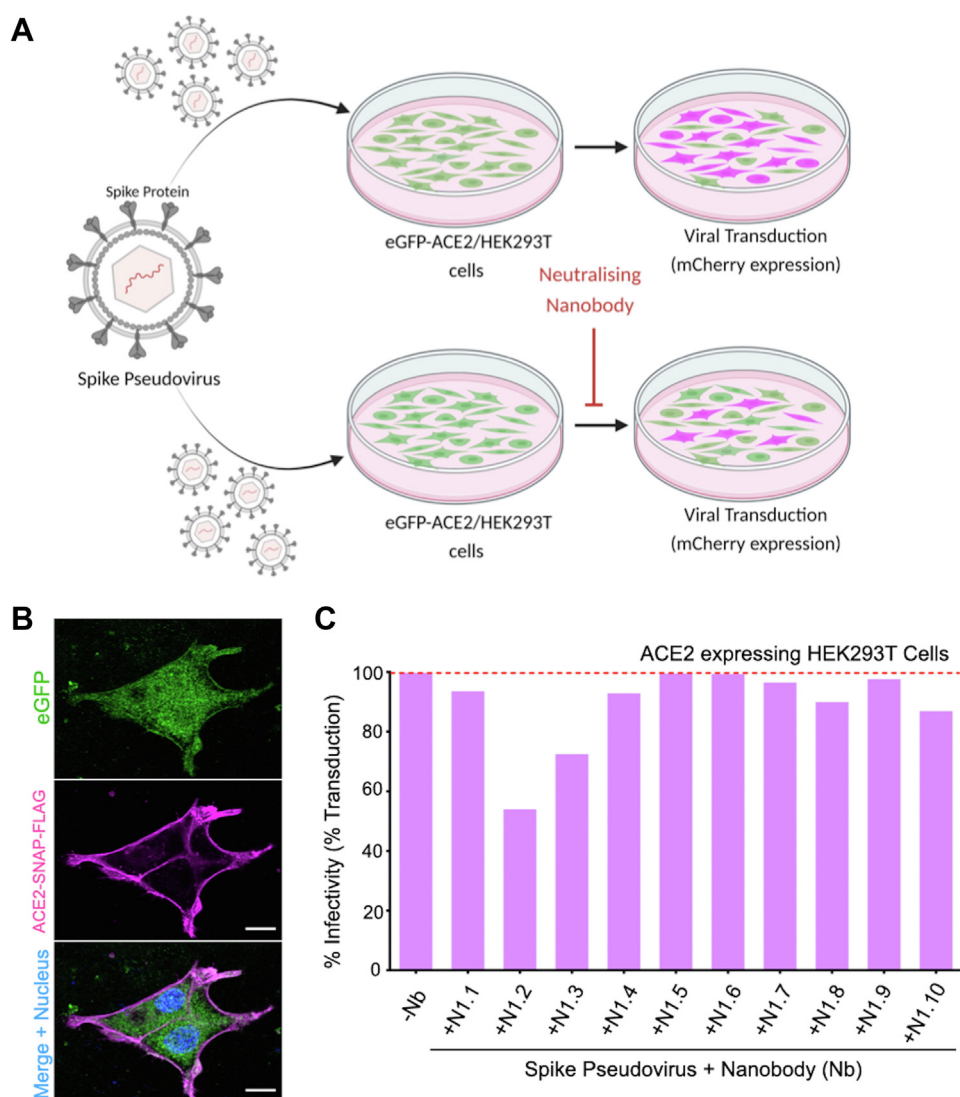
Figure 2. Characterization of nanobodies using virus entry assay. *A*, *cartoon* representation of the virus entry assay using spike pseudovirus. The pseudoviruses contain the mCherry gene in their genome and upon entering the eGFP-ACE2/HEK293T cell, the mCherry will be expressed and the fluorescence can be used for quantification of the virus infection. *B*, maximum intensity Z-projection of confocal images obtained from eGFP-ACE2/HEK293T, ACE2-SNAP-FLAG (*magenta*), eGFP (*green*), and nucleus (*blue*). The scale bar represents 10 microns. *C*, FACS-based quantification of spike pseudovirus infection into eGFP-ACE2/HEK293T (*magenta*) in the presence of various nanobodies as indicated (see the Experimental procedures section). The percentage of infectivity is normalized to the percentage of mCherry-positive cells in the absence of nanobody in the assay. For raw FACS data and details regarding the assay, refer to Fig. S4 and the Experimental procedures section. ACE2, angiotensin-converting enzyme 2; eGFP, enhanced GFP; FACS, fluorescent-activated cell sorting; HEK293T, human embryonic kidney 293T cell line.

About 25 μM of each nanobody, N1.1 to N1.10, was preincubated with the spike pseudovirus before infecting eGFP-ACE2/HEK293T cells (see the Experimental procedures section). Except for N1.2 and N1.3, all the nanobodies showed mCherry fluorescence (*i.e.*, no effect on pseudovirus entry) upon transduction in the eGFP-ACE2/HEK293T cells (Figs. 2C and S4). Interestingly, the N1.2 nanobody showed maximum efficiency in neutralizing the spike pseudoviruses compared with the remainder of the nanobodies (Fig. 2C). Therefore, we decided to further characterize the N1.2 nanobody as a potential nanobody against SARS-CoV-2 virus entry.

Microscopy-based cellular assay to assess N1.2

In our virus titration assays, we noticed that the FACS-based quantification does not scale according to the mCherry expression (Fig. S3, A and B). Therefore, we simultaneously correlated the mCherry fluorescence *versus* virus infection using confocal microscopy–based quantification (see the Experimental procedures section). In comparison to the FACS

data, the confocal microscopy–based measurement showed a sharp decline in mCherry fluorescence, that is, >80% decrease in mCherry fluorescence when 1/10th of the virus dilution was used for infection (Fig. S3, C–E). Therefore, hereafter, we used confocal microscopy–based measurement to assess the neutralizing potential of N1.2 nanobody against spike pseudovirus. In the pseudovirus assay, we used different concentrations of N1.2 (5, 10, and 25 μM) and could observe a linear reduction in the infectivity of the spike pseudoviruses in the eGFP-ACE2/HEK293T stable cell lines (Figs. 3, B, C and S5). To achieve a more potent inhibitory effect with N1.2, we engineered and purified a bivalent nanobody, in which the N1.2 sequence was placed in tandem, separated by a glycine–serine linker (see the Experimental procedures section) (Fig. S1 and Table S1). The tandem N1.2, termed as $(N1.2)_2$, showed a significant reduction in pseudoviral transduction at 5 and 10 μM concentrations (Fig. 3, B and C), suggesting a cooperative effect in neutralizing the spike pseudovirus.

To confirm if this inhibitory effect of N1.2 and $(N1.2)_2$ is achieved by its direct binding to spike envelope protein of
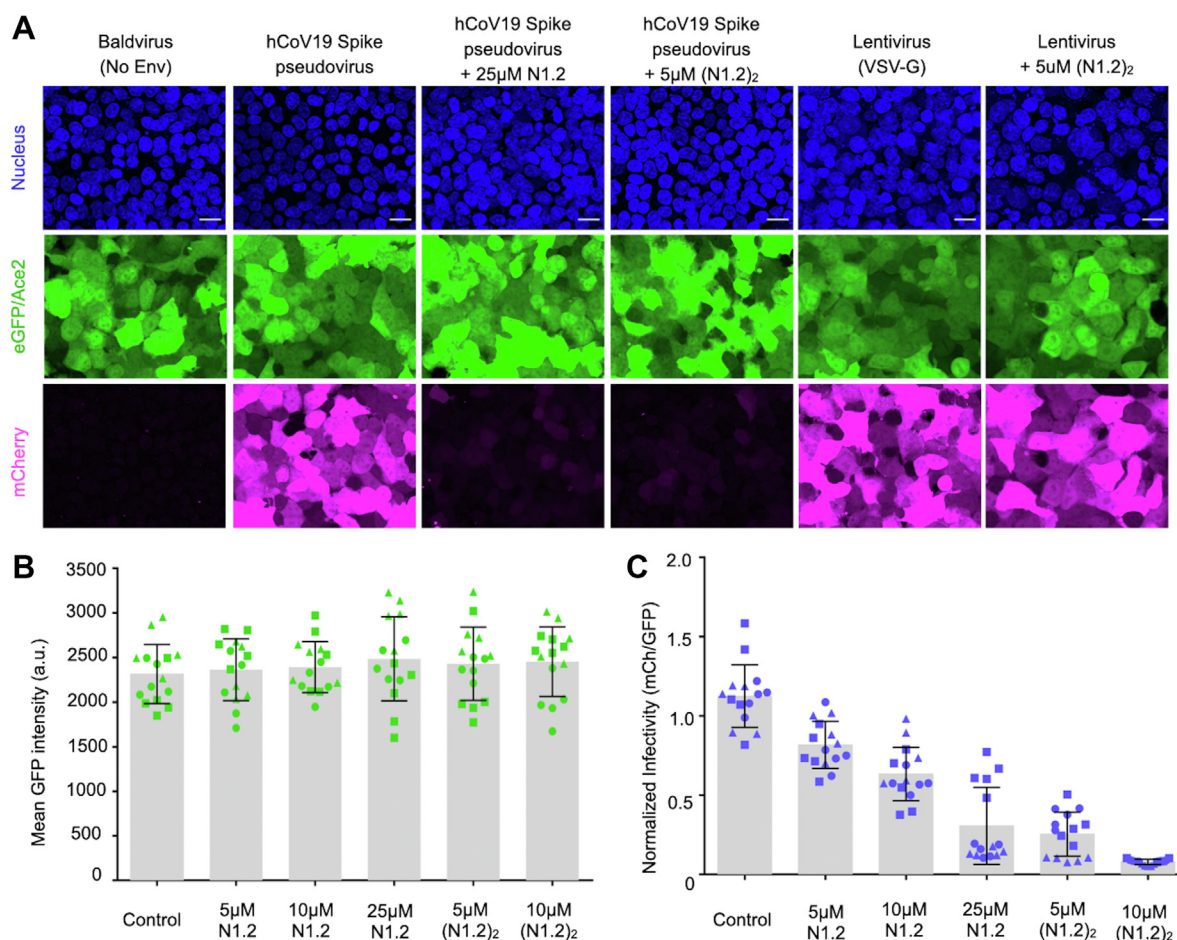
Figure 3. Assessing the efficacy of nanobody N1.2 using confocal microscopy. *A*, maximum intensity Z-projection of confocal images of bald and spike pseudovirus in the absence and presence of various concentrations of monovalent and bivalent nanobody N1.2 as indicated. The nucleus is shown in *blue*. The eGFP fluorescence (in *green*) is a proxy for ACE2 expression in HEK293T cells, and mCherry (in *magenta*) indicates the extent of virus entry into the eGFP-ACE2/HEK293T cells. The scale bar represents 20 microns. *B*, mean eGFP fluorescence from individual experiments as indicated, control group represents spike pseudovirus assay in the absence of nanobody. *C*, normalized infectivity quantified from mCherry over eGFP fluorescence for experiments with monovalent and bivalent nanobody N1.2 as indicated. For both *B* and *C*, data are shown as scatter plots with average values as *column bars*, where the mean was calculated from 15 data points from three independent experiments represented as *solid circles*, *squares*, and *triangles*, respectively. The error bars indicate the standard deviation. ACE2, angiotensin-converting enzyme 2; eGFP, enhanced GFP; HEK293T, human embryonic kidney 293T cell line.

SARS-CoV-2, we performed control experiments using vesicular stomatitis virus G (VSV-G) pseudoviruses and bald pseudoviruses (no glycoprotein-envelope control) (Figs. 3*A* and S5). These control VSV-G pseudoviruses transduce the stable cells similar to the spike pseudoviruses in the presence and absence of nanobody N1.2 or (N1.2)$_2$ (Fig. 3*A*). This indicates that the neutralizing effect of N1.2 and (N1.2)$_2$ is obtained by direct binding of the nanobody to the spike protein. Therefore, the engineered nanobody N1.2 can be effectively applied for antiviral therapy against coronavirus disease 2019.
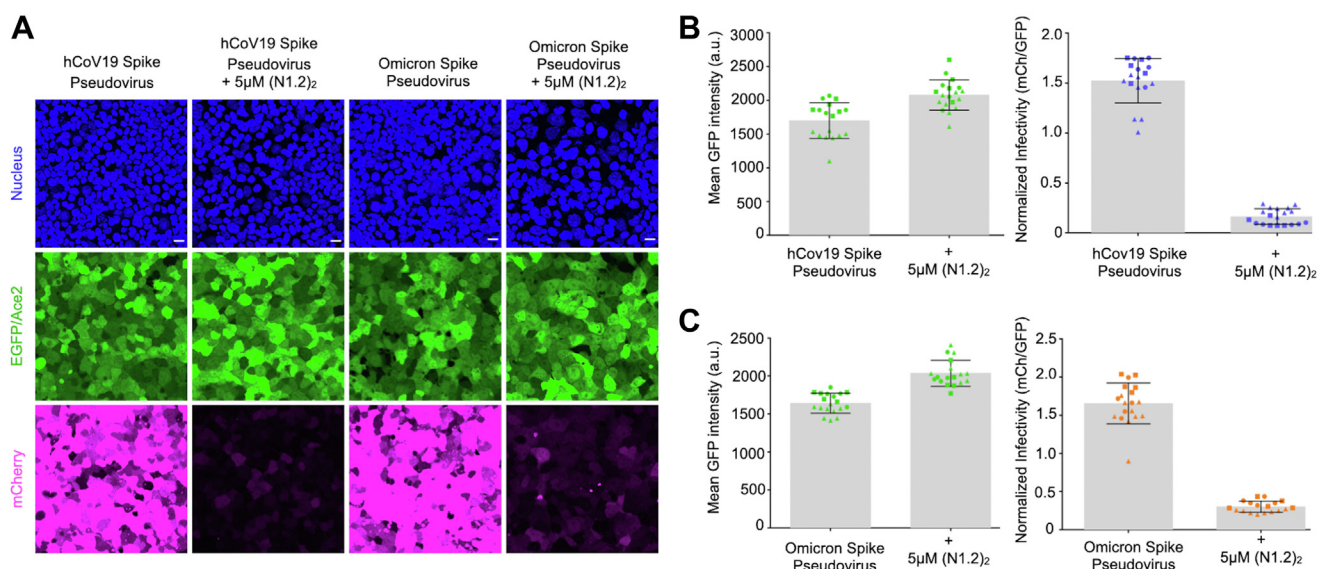
Efficacy of N1.2 against Omicron spike variant

We also tested the efficacy of the N1.2 against the newly emergent Omicron variant, using the Omicron BA.1 spike containing pseudoviruses expressing mCherry (see the Experimental procedures section). First, we confirmed the infectivity of varying concentrations of Omicron spike pseudovirus against eGFP-ACE2/HEK293T cells and determined an effective MOI (Fig. S3, *A* and *B*). Similar to the hCoV19 (Wuhan/WIV04/2019), the mCherry fluorescence was also scaled with the virus MOI for the Omicron variant spike pseudovirus in the confocal microscopy–based mCherry quantification (Fig. S3, *C–E*). We further tested the tandem nanobody (N1.2)$_2$ neutralizing effect against the Omicron spike pseudovirus in GFP-HEK293T (Fig. S6) and eGFP-ACE2/HEK293T (Fig. 4) (see the Experimental procedures section). The hCoV19 (Wuhan/WIV04/2019) and Omicron spike pseudovirus were efficiently blocked by 5 μM of (N1.2)$_2$ as observed from the confocal images in both cell lines (Figs. 4*A* and S6). Quantification of infectivity showed that in the presence of 5 μM of (N1.2)$_2$ the infectivity dropped to <10% (Fig. 4, *B* and *C*). Furthermore, it indicates the broad

neutralizing ability of the N1.2 nanobody reported here against the current SARS-CoV-2 Omicron variant.

Discussion

Since 2020, the SARS-CoV-2 virus has evolved into many subtypes and variants that are still prevalent across the globe (32). Therefore, it is pivotal to identify the broad-spectrum therapeutics that can effectively work against all SARS-CoV-2 subtypes and variants. Equally important is to establish validated pipelines that can expedite identifying new therapeutics against the emerging SARS-CoV-2 variants or new viruses. In this study, we have addressed both needs: first, we have identified a broad-spectrum nanobody that neutralizes the original Wuhan (WIV04) and Omicron BA.1 spike pseudovirus. Second, we have achieved the nanobody identification using a peptide as an antigen, unlike the whole spike or RBD protein of SARS-CoV-2 described earlier (13, 16, 33–35). The nanobodies or antibodies obtained by using a whole spike or RBD bind to different regions of the spike protein, and only a fraction of them were effective in neutralizing the virus (35), largely because these antibodies target the regions of the spike protein other than the ones involved in spike–ACE2 interaction. Peptides as antigens have been widely used for generating potent antibodies targeting the desired epitopes, for example, low-density lipoprotein receptor (36), hemagglutinin 1 of influenza virus (37), and SV40 virus (38), including the recent example for SARS-CoV-2 antibodies (39). These and several other examples suggest that the unstructured peptides can be highly antigenic and potentially yield antibodies that recognize the peptide epitopes in whole protein both in ordered and disordered states. However, peptides and flexible loops from a target protein have seldom been used as antigenic baits for

Figure 4. Comparison of nanobody N1.2 against hCoV19 and Omicron spike variant. *A*, maximum intensity Z-projection of confocal images of hCoV19 and Omicron spike pseudovirus in the presence of 5 μM bivalent nanobody (N1.2)$_2$ as indicated. The nucleus is shown in *blue*, the eGFP in *green*, and mCherry in *magenta*. The scale bar represents 20 microns. *B* and *C*, mean eGFP (*green*) and normalized infectivity quantification of hCoV19 (*blue*) and Omicron spike (*orange*) in the absence and presence of 5 μM bivalent nanobody (N1.2)$_2$ as indicated. For both *B* and *C*, the data are shown as scatter plots with average values as *column bars*, N = 18 data points from three independent experiments represented as *solid circles*, *squares*, and *triangles*, respectively. The error bars indicate the standard deviation. eGFP, enhanced GFP.

screening display libraries. We previously reported a nanobody against the tubulin post-translational modification using the flexible carboxy-terminal tail peptide (40). Applying a similar principle, here we show that a nine-amino acid peptide from the RBM of spike protein can also be employed as an epitope against a nanobody display library. The RBM adopts many conformations depending on the state of the apo spike protein and in complex with ACE2 (41), and in the absence of ACE2, the RBM appears to be unstructured (42). From our experiments, the nanobody is able to block the entry of SARS-CoV-2 spike pseudotyped virus, suggesting that the nanobody N1.2 could potentially recognize the unstructured RBM sequence. This approach of using synthetic peptide as an epitope instead of purified whole protein molecules will certainly accelerate and fine-tune the entire screening process, which will yield nanobodies/antibodies that are efficacious in neutralizing potential targets of viruses in the future.

The nanobody N1.2 described in this study is effective against both the spike proteins from the original hCoV19 (Wuhan/WIV04/2019) and the recent Omicron variant. Sequence alignment of the peptide-1 and its surrounding region shows the high similarity between the variants (Fig. S1D), suggesting that epitopes from the conserved RBM region, such as the peptide-1, can yield specific nanobodies or antibodies against the SARS-CoV-2 virus, yet possess broad neutralizing ability against the existing and emerging variants. Almost all the SARS-CoV-2 variants reported to date utilize ACE2 receptor binding for the host cell entry, and the RBM region of spike protein predominantly contributes to this interaction (43, 44). Therefore, we anticipate that the nanobody N1.2 will remain effective in neutralizing the emerging variants as long as the SARS-CoV-2 virus uses ACE2 for gaining entry into the host cells. In addition, the nanobodies offer advantages in engineering the valency and thereby increasing the efficacy in neutralization against the target molecules. Indeed, when we engineered the nanobody N1.2 into a bivalent version, (N1.2)$_2$, we observed a cooperative effect in neutralizing the pseudovirus even at the highest viral titers. Together, our study offers a platform to identify broad-spectrum nanobodies specific against SARS-CoV-2 and its variants, which can be exploited for other therapeutically relevant targets.

Experimental procedures

Peptide epitopes for screening

The peptide sequences were derived from two different regions of the RBM of spike proteins that have been crucial for the interaction of viral spike protein with the cellular ACE2 receptor. The following peptide sequences from the RBD of the spike were synthesized from LifeTein with a biotin tag:

Peptide-1: [FNCYFPLQS]S-K-Biotin
Peptide-2: Biotin-[GFQPTNGVGY]

Sequence alignment for coronavirus disease variants

The hCoV19 spike (Wuhan/WIV04/2019), GISAID (EPI_ISL_402124) construct is a kind gift from Prof Nevan Krogan, UCSF, United States (45). The sequence used for alignment was obtained from the National Center for Biotechnology Information GenBank. The accession number for Alpha (B1.1.7): MW487270.1, Delta (B1.617.2): OK091006.1, and BA.2: OM296922.1. The Omicron MC_0101274 was purchased from GenScript.

Screening yeast-display nanobody library of nanobodies

A combinatorial yeast-display library of nanobodies (NbLib) was obtained from Kerafast, Inc. The estimated diversity of the library is around $5 * 10^8$ unique nanobody clones expressed onto the surface of the yeast cells. The detailed protocol for screening nanobodies against the peptides has been adopted from the method described earlier (28). The frozen vial of NbLib (fivefold excess of library diversity) was grown in 1 l Yglc4.5-Trp media (3.8 g/l of −Trp drop-out media supplement, 6.7 g/l yeast nitrogen base, 10.4 g/l sodium citrate, 7.4 g/l citric acid monohydrate, 20 g/l glucose, and 10 ml/l PenStrep, pH 4.5) at 30 °C for 24 to 48 h and passaged thrice before the screening. The freshly passaged NbLib ($5 * 10^9$ cells, 10-fold excess of library) was induced in galactose containing media (−Trp +galactose; 3.8 g/l of −Trp drop-out media supplement, 6.7 g/l yeast nitrogen base, 20 g/l galactose, and 10 ml/l PenStrep, pH 6.0) at 20 °C for 72 h to achieve sufficient expression in the library.

Magnetic selection

Around $5 * 10^9$ nanobody-expressing yeast cells were pelleted to remove media and washed with 10 ml selection buffer (20 mM Hepes [pH 7.5], 150 mM sodium chloride, 0.1% [w/v] bovine serum albumin, and 5 mM maltose). The cells were resuspended in 4.5 ml of selection buffer. First, we performed negative magnetic selection (MACS) by incubating the aforementioned, resuspended cells with 200 μl of antibiotin microbeads (Miltenyi Biotec; catalog no.: 130-090-485) and 200 μl of streptavidin microbeads (Miltenyi Biotec; catalog no.: 130-048-102) at 4 °C for 1 h. Postincubation, the cells were pelleted, resuspended in 5 ml selection buffer, and were allowed to pass through (*via* gravity flow) the LD column (Miltenyi Biotec; catalog no.: 130-042-901) placed on Miltenyi MACS magnet (using Midi MACS separator) pre-equilibrated with 5 ml selection buffer. The unbound cells were collected, and the column was washed with an additional 2 ml of the selection buffer to flush out the remaining cells from the column. The cells were pelleted and resuspended in a 3 ml selection buffer for positive selection with the peptides.

First MACS selection

The cells were incubated with a 10 μM concentration of peptide-1/peptide-2 at 4 °C for 1 h, following which 100 μl of antibiotin microbeads were added and incubated for an additional 20 min at 4 °C. The cells were pelleted and washed with a 3 ml selection buffer. The cells were resuspended in a 3 ml selection buffer and passed through the pre-equilibrated (with 5 ml selection buffer) LS column (Miltenyi Biotec; catalog no.: 130-042-401) placed on the Miltenyi MACS magnet. The LS column was washed with an additional 8 ml of the selection

buffer to remove unbound cells from the column. The column was removed from the magnet and added 3 ml of the selection buffer to the column. Using a plunger, all the bound yeast cells from the column were eluted in 50 ml falcon. The cells were pelleted and resuspended in –Trp +glucose media (3.8 g/l of –Trp drop-out media supplement, 6.7 g/l yeast nitrogen base, 20 g/l glucose, and 10 ml/l PenStrep, pH 6.0) for growth at 30 °C for 48 h.

Second MACS selection

Took 10^9 first magnetic sorted cells and induced them in –Trp +galactose media for 72 h. Around 10^8 freshly induced yeast cells were taken and pelleted. The cells were washed with a 5 ml selection buffer and resuspended in a 3 ml selection buffer. Added 10 µM of the respective peptide and incubated at 4 °C for 1 h. To this, added 100 µl of streptavidin microbeads and incubated for an additional 20 min at 4 °C. The cells were pelleted, washed with 3 ml selection buffer, and resuspended in 3 ml of selection buffer to pass them through the pre-equilibrated LS column placed on the Miltenyi MACS magnet. Washed the column with 8 ml additional selection buffer, followed which the column was removed from the magnet and plunged all the bead-bound cells from the column by 3 ml selection buffer. The cells were pelleted and resuspended in 5 ml –Trp +glucose media and kept for growth at 30 °C for 48 h.

FACS

Finally, the second MACS sorted culture was induced (around 10^9 cells) in galactose media at 20 °C for 72 h and performed cell sorting experiments to enrich the high-affinity nanobody against the target peptides. Here, we took 10^7 cells and pelleted them in a microcentrifuge vial. These cells were washed with 1 ml selection buffer and resuspended the cells in 100 µl selection buffer. The cells were incubated with 100 µM of the respective peptide and 1:200 dilution of rabbit anti-hemagglutinin tag antibody (Sigma; catalog no.: H6908) at 4 °C for 1 h. Cells were washed with 1 ml selection buffer and resuspended in 100 µl of selection buffer for secondary antibody staining. Cells were incubated with 1:200 dilution of goat anti-rabbit Alexa Fluor-647 antibody (Invitrogen) and 1:100 dilution of neutravidin fluorescein conjugate (Invitrogen; FITC; catalog no.: A2662; used for the first FACS) at 4 °C for 30 min. Post-incubation, cells were washed twice with a 1 ml selection buffer to remove unbound reagents. Cells were resuspended in 1 ml selection buffer just before sorting them on BD FACS Aria Fusion for double-positive cells, keeping unstained and single stained controls (Central Imaging and Flow Cytometry Facility at the National Centre for Biological Sciences). About 0.1 to 1% of the cells, positive for both the fluorophores (for neutravidin-FITC and Alexa Fluor 647 fluorophores), which are represented as the P2 population in the Q2 quadrant of the sorting layout. A total of around 8000 to 10,000 cells were collected and grown in 5 ml fresh –Trp +glucose media at 30 °C for 48 h. The freshly grown cells were propagated in larger volumes in the same glucose media (250–500 ml) to make stocks (–Trp +glucose media and 10% dimethyl sulfoxide) and further characterize

individual clones for their affinity with the respective peptide. After the sorting experiment, the cells were plated onto an agar plate (–Trp +glucose +15 g/l agar), and 10 single yeast colonies of postsorted cultures were analyzed on a flow cytometer (Thermo, Attune) for their binding with the respective peptide. Only peptide-1 screening yielded nanobody clones from the library having sufficient binding affinity for peptide-1; therefore, we have only focused on characterizing nanobodies obtained from peptide-1 screening. We have isolated plasmids from these 10 individual yeast clones from peptide-1 screening to identify the protein-coding sequences of these nanobodies for cellular validation.

Cloning and protein purification

The nanobody gene was amplified from isolated yeast colonies and cloned between HindIII and XhoI sites in a pET-22b (+) plasmid containing a C-terminal 6× histidine tag.

The N1.2 nanobody sequence was first cloned with Linker AS-$(G_4S)_3$-G in a cytomegalovirus vector (backbone from Addgene; #12298) using 5′-tccggtggcggaggctccggtggcggaggtt ccggacaggtgcagctgcaggaaagcgg-3′ and 5′-cacactggatcagttatc-tatgcggccgctcagtggtggtggtggtggtgctcgaggc-3′ primers. The sequence of N1.2 along with the AS$(G_4S)_3$G linker was amplified using 5′-gccagggcacccaggtgaccgtgagcagcgctagcggt ggtggaggctccggtggcggaggc-3′ and 5′-cagccggatctcagtggtgg tggtggtggtgctcgaggctgctcacggtcacctgggtgccc-3′ primers. This amplified construct of linker-N1.2 was cloned in pet22B amplified vector (5′-cggagcctccaccaccgctagcgctgctcacggt-cacctgggtgccc-3′ and 5′-tcgagcaccaccaccaccaccactgagatcc ggctgctaac-3′) already cloned with N1.2 sequence (between NcoI and XhoI) using Gibson assembly method. The resulting construct contains an amino-terminal pelB sequence, two tandem sequences of N1.2 spaced with AS$(G_4S)_3$G linker, and a C-terminal 6× histidine tag.

The nanobodies were purified from Rosetta (DE3) cells in an LB medium by inducing at an absorbance of 0.5 with 0.5 mM IPTG at 20 ˚C. After overnight induction, the cells were pelleted down and the protein was extracted by osmotic shock by resuspending in 0.5 M sucrose, 0.2 M Tris, pH 8, 0.5 mM EDTA, followed by water in a 1:3 ratio with 1 h of stirring at 4 °C. The lysate was adjusted to contain 150 mM NaCl, 2 mM $MgCl_2$, and 20 mM imidazole and was subjected to centrifugation at 18,000 RPM at 4 °C to remove cell debris. The supernatant was loaded on 5 ml HisTrap HP (GE Healthcare). The column was subsequently washed by high salt buffer (20 mM Tris [pH 8] and 500 mM NaCl) and low imidazole buffer (20 mM Tris [pH 8], 100 mM NaCl, 100 mM imidazole, pH 8). The protein was eluted with 20 mM Tris, 100 mM NaCl, and 400 mM imidazole (pH 8). The eluted protein was concentrated in 3 KDa cutoff centricon (UFC9003) and buffer exchanged (20 mM Tris [pH 8] and 100 mM NaCl). The protein was aliquoted, flash-frozen, and stored at –80 °C (28).

Cell culture experiments

Wildtype mammalian HEK293T cells and LentiX-293T cells (Takara Bio; catalog no.: 632180) were used in this study for

pseudotyped spike virus production and viral transduction assay. Both these cell lines were grown in Dulbecco's modified Eagle's medium (DMEM) (Thermo Fisher Scientific; catalog no.: 11995065) supplemented with 10% fetal bovine serum, 1× PenStrep (Gibco; Thermo Fisher Scientific; catalog no.: 15-140-122), and 1× GlutaMAX (Gibco; catalog no.: 35050061) in a humidified 37 °C incubator with 5% CO_2 supply.

Spike pseudotyped virus production

Freshly passaged HEK293T cells were seeded in a 100 mm cell culture plate and grown up to 70 to 80% confluency. The media of the cells were changed to 10 ml complete DMEM without PenStrep before transfection. For viral particle production, 5 μg pHR lentiviral vector cloned with mCherry fluorescent protein, 3.75 μg packaging plasmid psPAX2 (Addgene; #12260), and 2.5 μg envelope plasmid for the expression of spike glycoprotein (obtained as a kind gift from Prof Nevan Krogan, UCSF) of SARS-CoV-2 were mixed in 500 μl OptiMEM media and 20 μl PLUS reagent (Invitrogen; LTX transfection reagent; catalog no.: L15338100) and kept for incubation at room temperature for 5 min. In a separate microcentrifuge vial, 500 μl OptiMEM was taken, and 30 μl Lipofectamine-LTX reagent was added to it. This Lipofectamine-containing solution was added to the plasmid and incubated at room temperature for 20 min. We also generated control lentiviral particles by replacing spike plasmid with VSV-G envelope protein, pmDG2 (Addgene; #12259) plasmid. The aforementioned transfection mix was added to the cells and post 16 to 18 h; the media were changed to PenStrep containing complete DMEM. The viral supernatant was collected at 48, 72, and 96 h post-transfection by replacing 10 ml fresh media every time. All the viral supernatants were pooled together and stored at 4 °C till 96 h post-transfection. The supernatant was concentrated up to ∼1 to 3 ml using a 50-KDa Millipore Amicon filter (Merck; UFC905024) at 1000*g* and 4 °C. The concentrated viral supernatant was mixed with one-third volume of Lenti-X concentrator (Takara Bio; catalog no.: 631231) overnight at 4 °C and pelleted at 1500*g* for 45 min at 4 °C. The off-white pellet of the viruses was resuspended in 1 to 2 ml of complete DMEM (10% fetal bovine serum) and stored at –80 °C in 100 to 200 μl aliquots until further use.

Omicron pseudotyped virus production

Omicron pseudotyped viruses were produced similarly as described previously for spike pseudoviruses but instead used Omicron envelope plasmid along with packaging plasmid (psPAX2) and lentiviral plasmid (pHR mCherry) in the following ratio: psPAX2 (1.3 pmol), pHR mCherry: 1.64 pmol, SARS-CoV-2 Omicron Strain S gene (GenScript; catalog no.: MC_0101274): 0.72 pmol.

Cloning of ACE2 in lentiviral vector (pTRIP vector)

Human *ACE2* was amplified from the mammalian Caco2 cell lines. Caco2 cells were lysed for total RNA purification

using the Trizol method. Furthermore, 2 μg of total RNA was set up for complementary DNA (cDNA) synthesis with Verso cDNA synthesis kit (Thermo Fisher Scientific; catalog no.: AB1453A) as per the manufacturer's protocol. The protein-coding sequence of ACE2 was amplified from the cDNA with forward (5′-ggaggagaaccctggacctggatccatgtcaa gctcttcctggctcc-3′) and reverse (5′-ctcctgaccctcctcccccg- taaaaggaggtctgaacatc-3′) primers using Q5 polymerase PCR (NEB; catalog no.: M0492L). This amplified construct of *ACE2* was cloned into a pTRIP chicken β-actin (CAG) vector (46). This construct contains amino-terminal eGFP followed by self-cleaving 2A peptide sequence followed by *ACE2* and carboxy-terminal SNAP-tag and FLAG tags (eGFP-ACE2/ HEK293T).

Generation of stable HEK293T cell line for overexpression of ACE2

The lentiviral pTRIP vector cloned with eGFP-ACE2/ HEK293T under cytomegalovirus enhancer and chicken β-actin promoter (CAG promoter) flanked with 5 and 3′ long terminal repeat sequences (46) was used to produce lentiviral particles as per the method described before (40). Briefly, 70 to 80% confluent HEK293T cells were transfected with 5 μg lentiviral construct of eGFP-ACE2-SNAP-FLAG, 3.75 μg psPAX2 (Addgene; #12260), and 2.5 μg pmDG2 (Addgene; #12259) plasmids using Lipofectamine-LTX reagent. The lentiviruses collected at 48, 72, and 96 h were concentrated and pelleted using a Lenti-X concentrator. The white pellet of lentiviruses was resuspended in 2 ml of complete DMEM, and 1 ml of this virus was used to transduce HEK293T cells for stable expression of ACE2 in these cells. We could only achieve the transduction efficiency of 60 to 70%, and therefore, we performed FACS experiments to enrich the eGFP expressing (a proxy for ACE2 expression) HEK293T cells in the culture. In our sorted culture, >90% of cells were found to be eGFP positive or expressing eGFP-ACE2.

Immunofluorescence assay for ACE2 expression

The stable HEK293T cells were seeded in ibidi glass-bottom dishes (catalog no.: 81218) precoated with poly-D-lysine and grown to 70% confluency. The cells were washed with 1× BRB80 (80 mM Pipes, 1 mM $MgCl_2$, and 1 mM EGTA, pH 6.8) buffer twice and fixed using 100% ice-cold methanol for 10 min at –20 °C. Postfixation, cells were washed twice with 1× BRB80 buffer and permeabilized in the same buffer having 0.1% Triton X-100 for 10 min at room temperature. Cells were blocked with 5% bovine serum albumin (BSA) made in 1× BRB80 + 0.1% Triton X-100 for 1 h at room temperature. Cells were incubated with 1:500 dilution of mouse anti-FLAG monoclonal antibody (Merck; catalog no.: F3165) overnight at 4 °C. Furthermore, cells were washed thrice for 5 min using a blocking buffer, followed by secondary goat antimouse Alexa Fluor-647 antibody (Invitrogen; 1:1000 dilution) incubation in the same blocking buffer at room temperature for 2 h. Cells were stained for nucleus using 4′,6-diamidino-2-phenylindole (1 μg/ml) for 10 min followed by five washes with 1× BRB80

for 5 min. Cells were imaged on an H-TIRF microscope using 405, 488, and 640 nm laser with appropriate filter sets.

Immunoblotting assay for ACE2 expression

The HEK293T cells were seeded in a 35 mm dish grown to 70% confluency. The cells were transfected with 1 μg of eGFP-ACE2-SNAP-FLAG with Jet Prime reagent for 24 and 48 h. Cells were lysed with radioimmunoprecipitation assay buffer and subjected to 12% SDS-PAGE. The wet transfer was performed on methanol-activated polyvinylidene difluoride membrane for 75 min at 100 V at 4 °C. The blots were probed with 1:5000 anti-FLAG antibody (Sigma; F3165) overnight at 4 °C followed by 1:10,000 antimouse secondary at room temperature for 1 h. The blots were developed by chemiluminescence on iBright1500 (Invitrogen) by Pierce ECL substrate (Thermo Fisher Scientific; catalog no.: 32106).

ELISA

The surface of the 96-well plates was passivated with BSA–biotin (Thermo Fisher Scientific; catalog no.: 29130; 1 mg/ml, 5 min), followed by a 1× PBS wash. The surface was coated with 0.5 mg/ml streptavidin (Thermo Fisher Scientific; catalog no.: 43-4302) for 5 min and washed twice with 1× PBS (8 g/l NaCl, 0.2 g/l KCl, 1.44 g/l Na_2HPO_4, 0.24 g/l KH_2PO_4, pH 7.4). The surface was immobilized with a 200 μM biotinylated peptide-1/peptide-2 sequence for 30 min on ice. The well surface was blocked with 5% BSA containing 1× PBS for 1 h on ice. All the nanobodies (containing carboxy-terminal 6× His tag) screened for peptide-1 were diluted in blocking buffer at 10 μM concentration and incubated with the immobilized peptides for 1 h on ice. The surface of the well was washed twice with blocking buffer and incubated with horseradish peroxidase–conjugated rabbit anti-6xHis tag antibody (Abcam; catalog no.: AB1187), 1:10,000 dilution at 4 °C overnight. The wells were washed thrice with the blocking buffer and incubated with 100 μl of 1:10 diluted (diluted in distilled water) 3,3′,5,5′-tetramethylbenzidine substrate solution (Thermo Fisher Scientific; catalog no.: N301). Once the color starts to develop, stop the reaction using 0.2 mM sulfuric acid. The color will turn yellow upon sulfuric acid addition, which was measured for absorbance at 450 nm using a spectrophotometer keeping appropriate controls (wells not having any immobilized peptides). The intensity of the yellow color represents the binding of nanobodies with the respective peptide. The relative absorbance (at 450 nm) values of individual nanobodies plotted in the graph represent absorbance at 450 nm with peptide subtracted from absorbance at 450 nm without peptide.

Pseudoviral transduction assay

The GFP/HEK293T cells or eGFP-ACE2/HEK293T cells were grown up to 60 to 70% confluency in complete media before viral transduction. In a separate vial, mCherry pseudoviruses/lentiviruses were incubated with the respective purified nanobody at room temperature for 5 min. The cells were transduced with the aforementioned viral mix along with 2 μg/ml Polybrene (Merck; catalog no.: TR-1003-G) overnight (12–15 h), keeping appropriate positive and negative controls. After viral incubation, cells were grown in complete media for 48 h and then processed for flow cytometric analysis and confocal imaging.

In this assay, the viral titer was used in a concentration such that to obtain more than 70% transduction efficiency in the eGFP-ACE2/HEK293T or eGFP/HEK293T cell line. We have used 10 μl of spike pseudoviruses and 4 μl Omicron pseudoviruses for flow cytometry and microscopy experiments. For flow cytometric analysis, cells were resuspended in 1× PBS and were subjected to Attune NxT Acoustic Focusing Cytometer to measure *red* (mCherry) and *green* (eGFP-ACE2/HEK293T) fluorescence using YL2 (620/15 nm) and BL1 (530/30 nm) filters. Confocal imaging was performed to quantitate the mCherry expression in the stable HEK293T cells after pseudoviral transduction in the presence and absence of the N1.2 and $(N1.2)_2$ nanobodies.

Quantification of percentage transduction of cells with pseudovirus (spike and Omicron) was done on BD LSRFortessa using 488 and 561 lasers with 530/30 (505LP) and 610/20 (600LP), respectively.

Imaging and statistical analysis

All the images were acquired on an inverted confocal microscope (Olympus FV3000) equipped with six solid-state laser lines (405, 445, 488, 514, 561, and 640 nm) and a 20× oil objective. For the acquisition and quantification of viral transduction in the pseudoviral assay, high-sensitivity spectral detectors were used marking a specific region of interest in the 2048 * 2048 pixel frame. For all the sets of images acquired for quantification, laser power, voltage, and gain settings were kept constant. Images were analyzed on Fiji software ([47](#)) to calculate mean fluorescence intensity for eGFP (ACE2 expression) and mCherry (viral transduction) channels from the z-projected stacks. All the experiments were performed in triplicate sets on at least two different days. Normalized infectivity represents the mean mCherry intensity of a particular z-projected stack over the GFP intensity of the same stacks. Representative images are the z-projected stacks of the respective condition. eGFP-ACE2/HEK293T immunostained with FLAG antibody was imaged at 60× oil objective of FV3000 confocal microscope ([Fig. 2*B*](#)) and 100× oil objective of H-TIRF microscope ([Fig. S2*A*](#)) using 405, 488, and 647 nm laser lines for 4′,6-diamidino-2-phenylindole, eGFP, and Alexa Fluor-647 fluorophores.

Data availability

All the data generated during the study are included in the main text and supporting information.

Broad-spectrum nanobody neutralizing SARS-CoV-2 variants

References

1. Tang, D., Comish, P., and Kang, R. (2020) The hallmarks of COVID-19 disease. *PLoS Pathog.* **16**, e1008536
2. Xu, Z., Liu, K., and Gao, G. F. (2022) Omicron variant of SARS-CoV-2 imposes a new challenge for the global public health. *Biosaf. Health.* https://doi.org/10.1016/j.bsheal.2022.01.002
3. Cobey, S., Larremore, D. B., Grad, Y. H., and Lipsitch, M. (2021) Concerns about SARS-CoV-2 evolution should not hold back efforts to expand vaccination. *Nat. Rev. Immunol.* **21**, 330–335
4. He, Y., Lu, H., Siddiqui, P., Zhou, Y., and Jiang, S. (1950) (2005) Receptor-binding domain of severe acute respiratory syndrome coronavirus spike protein contains multiple conformation-dependent epitopes that induce highly potent neutralizing antibodies. *J. Immunol. Baltim. Md.* **174**, 4908–4915
5. Lan, J., Ge, J., Yu, J., Shan, S., Zhou, H., Fan, S., *et al.* (2020) Structure of the SARS-CoV-2 spike receptor-binding domain bound to the ACE2 receptor. *Nature.* https://doi.org/10.1038/s41586-020-2180-5
6. Walls, A. C., Park, Y.-J., Tortorici, M. A., Wall, A., McGuire, A. T., and Veesler, D. (2020) Structure, function, and antigenicity of the SARS-CoV-2 spike glycoprotein. *Cell* **181**, 281–292.e6
7. Shang, J., Wan, Y., Luo, C., Ye, G., Geng, Q., Auerbach, A., *et al.* (2020) Cell entry mechanisms of SARS-CoV-2. *Proc. Natl. Acad. Sci. U. S. A.* **117**, 11727–11734
8. Custódio, T. F., Das, H., Sheward, D. J., Hanke, L., Pazicky, S., Pieprzyk, J., *et al.* (2020) Selection, biophysical and structural analysis of synthetic nanobodies that effectively neutralize SARS-CoV-2. *Nat. Commun.* **11**, 5588
9. Hanke, L., Vidakovics Perez, L., Sheward, D. J., Das, H., Schulte, T., Moliner-Morro, A., *et al.* (2020) An alpaca nanobody neutralizes SARS-CoV-2 by blocking receptor interaction. *Nat. Commun.* **11**, 4420
10. Huo, J., Bas, A. L., Ruza, R., Duyvesteyn, H. M. E., Mikolajek, H., Malinauskas, T., *et al.* (2020) Structural characterisation of a nanobody derived from a naïve library that neutralises SARS-CoV-2. *Res. Square.* https://doi.org/10.21203/rs.3.rs-32948/v1
11. Mast, F. D., Fridy, P. C., Ketaren, N. E., Wang, J., Jacobs, E. Y., Olivier, J. P., *et al.* (2021) Highly synergistic combinations of nanobodies that target SARS-CoV-2 and are resistant to escape. *eLife* **10**, e73027
12. Shi, R., Shan, C., Duan, X., Chen, Z., Liu, P., Song, J., *et al.* (2020) A human neutralizing antibody targets the receptor-binding site of SARS-CoV-2. *Nature* **584**, 120–124
13. Wang, C., Li, W., Drabek, D., Okba, N. M. A., van Haperen, R., Osterhaus, A. D. M. E., *et al.* (2020) A human monoclonal antibody blocking SARS-CoV-2 infection. *Nat. Commun.* **11**, 2251
14. Wrapp, D., De Vlieger, D., Corbett, K. S., Torres, G. M., Wang, N., Van Breedam, W., *et al.* (2020) Structural basis for potent neutralization of betacoronaviruses by single-domain camelid antibodies. *Cell* **181**, 1436–1441
15. Xiang, Y., Nambulli, S., Xiao, Z., Liu, H., Sang, Z., Duprex, W. P., *et al.* (2020) Versatile and multivalent nanobodies efficiently neutralize SARS-CoV-2. *Science* **370**, 1479–1484
16. Ye, M., Fu, D., Ren, Y., Wang, F., Wang, D., Zhang, F., *et al.* (2020) Treatment with convalescent plasma for COVID-19 patients in Wuhan, China. *J. Med. Virol.* **92**, 1890–1901
17. Schoof, M., Faust, B., Saunders, R. A., Sangwan, S., Rezelj, V., Hoppe, N., *et al.* (2020) An ultrapotent synthetic nanobody neutralizes SARS-CoV-2 by stabilizing inactive Spike. *Science* **370**, 1473–1479
18. B, Z., S, L., T, T., W, H., Y, D., L, C., *et al.* (2020) Treatment with convalescent plasma for critically Ill patients with severe acute respiratory syndrome coronavirus 2 infection. *Chest.* https://doi.org/10.1016/j.chest.2020.03.039
19. Cao, Y., Su, B., Guo, X., Sun, W., Deng, Y., Bao, L., *et al.* (2020) Potent neutralizing antibodies against SARS-CoV-2 identified by high-throughput single-cell sequencing of convalescent patients' B cells. *Cell* **182**, 73–84.e16
20. Minenkova, O., Santapaola, D., Milazzo, F. M., Anastasi, A. M., Battistuzzi, G., Chiapparino, C., *et al.* (2022) Human inhalable antibody fragments neutralizing SARS-CoV-2 variants for COVID-19 therapy. *Mol. Ther.* https://doi.org/10.1016/j.ymthe.2022.02.013
21. Shen, C., Wang, Z., Zhao, F., Yang, Y., Li, J., Yuan, J., *et al.* (2020) Treatment of 5 critically Ill patients with COVID-19 with convalescent plasma. *JAMA* **323**, 1582–1589
22. Wu, X., Cheng, L., Fu, M., Huang, B., Zhu, L., Xu, S., *et al.* (2021) A potent bispecific nanobody protects hACE2 mice against SARS-CoV-2 infection *via* intranasal administration. *Cell Rep.* **37**, 109869
23. Ye, G., Gallant, J., Zheng, J., Massey, C., Shi, K., Tai, W., *et al.* (2021) The development of Nanosota-1 as anti-SARS-CoV-2 nanobody drug candidates. *eLife* **10**, e64815
24. Muyldermans, S. (2013) Nanobodies: natural single-domain antibodies. *Annu. Rev. Biochem.* **82**, 775–797
25. Bannas, P., Hambach, J., and Koch-Nolte, F. (2017) Nanobodies and nanobody-based human heavy chain antibodies as antitumor therapeutics. *Front. Immunol.* **8**, 1603
26. Vincke, C., Loris, R., Saerens, D., Martinez-Rodriguez, S., Muyldermans, S., and Conrath, K. (2009) General strategy to humanize a camelid single-domain antibody and identification of a universal humanized nanobody scaffold. *J. Biol. Chem.* **284**, 3273–3284
27. Ghorbani, M., Brooks, B. R., and Klauda, J. B. (2021) Exploring dynamics and network analysis of spike glycoprotein of SARS-COV-2. *Biophys. J.* **120**, 2902–2913
28. McMahon, C., Baier, A. S., Pascolutti, R., Wegrecki, M., Zheng, S., Ong, J. X., *et al.* (2018) Yeast surface display platform for rapid discovery of conformationally selective nanobodies. *Nat. Struct. Mol. Biol.* **25**, 289–296
29. Chen, M., and Zhang, X.-E. (2021) Construction and applications of SARS-CoV-2 pseudoviruses: a mini review. *Int. J. Biol. Sci.* **17**, 1574–1580
30. Hoffmann, M., Kleine-Weber, H., Schroeder, S., Krüger, N., Herrler, T., Erichsen, S., *et al.* (2020) SARS-CoV-2 cell entry depends on ACE2 and

TMPRSS2 and is blocked by a clinically proven protease inhibitor. *Cell* **181**, 271–280.e8

31. [preprint] Sherman, E. J., and Emmer, B. T. (2021) ACE2 protein expression within isogenic cell lines is heterogeneous and associated with distinct transcriptomes. *bioRxiv*. https://doi.org/10.1101/2021.03.26.437218

32. Harvey, W. T., Carabelli, A. M., Jackson, B., Gupta, R. K., Thomson, E. C., Harrison, E. M., *et al.* (2021) SARS-CoV-2 variants, spike mutations and immune escape. *Nat. Rev. Microbiol.* **19**, 409–424

33. Du, L., Yang, Y., and Zhang, X. (2021) Neutralizing antibodies for the prevention and treatment of COVID-19. *Cell Mol. Immunol.* **18**, 2293–2306

34. Papageorgiou, A. C., and Mohsin, I. (2020) The SARS-CoV-2 spike glycoprotein as a drug and vaccine target: structural insights into its complexes with ACE2 and antibodies. *Cells* **9**, E2343

35. Yu, F., Xiang, R., Deng, X., Wang, L., Yu, Z., Tian, S., *et al.* (2020) Receptor-binding domain-specific human neutralizing monoclonal antibodies against SARS-CoV and SARS-CoV-2. *Signal. Transduct. Target. Ther.* **5**, 212

36. Schneider, W. J., Slaughter, C. J., Goldstein, J. L., Anderson, R. G., Capra, J. D., and Brown, M. S. (1983) Use of antipeptide antibodies to demonstrate external orientation of the NH2-terminus of the low density lipoprotein receptor in the plasma membrane of fibroblasts. *J. Cell Biol.* **97**, 1635–1640

37. Green, N., Alexander, H., Olson, A., Alexander, S., Shinnick, T. M., Sutcliffe, J. G., *et al.* (1982) Immunogenic structure of the influenza virus hemagglutinin. *Cell* **28**, 477–487

38. Walter, G., Scheidtmann, K. H., Carbone, A., Laudano, A. P., and Doolittle, R. F. (1980) Antibodies specific for the carboxy- and amino-terminal regions of simian virus 40 large tumor antigen. *Proc. Natl. Acad. Sci. U. S. A.* **77**, 5197–5200

39. Traboulsi, H., Khedr, M. A., Al-Faiyz, Y. S. S., Elgorashe, R., and Negm, A. (2021) Structure-based epitope design: toward a greater antibody-SARS-CoV-2 RBD affinity. *ACS Omega* **6**, 31469–31476

40. Kesarwani, S., Lama, P., Chandra, A., Reddy, P. P., Jijumon, A. S., Bodakuntla, S., *et al.* (2020) Genetically encoded live-cell sensor for tyrosinated microtubules. *J. Cell Biol.* **219**, e201912107

41. Xu, C., Wang, Y., Liu, C., Zhang, C., Han, W., Hong, X., *et al.* (2021) Conformational dynamics of SARS-CoV-2 trimeric spike glycoprotein in complex with receptor ACE2 revealed by cryo-EM. *Sci. Adv.* **7**, eabe5575

42. Williams, J. K., Wang, B., Sam, A., Hoop, C. L., Case, D. A., and Baum, J. (2022) Molecular dynamics analysis of a flexible loop at the binding interface of the SARS-CoV-2 spike protein receptor-binding domain. *Proteins Struct. Funct. Bioinforma.* **90**, 1044–1053

43. Sanches, P. R. S., Charlie-Silva, I., Braz, H. L. B., Bittar, C., Freitas Calmon, M., Rahal, P., *et al.* (2021) Recent advances in SARS-CoV-2 Spike protein and RBD mutations comparison between new variants Alpha (B.1.1.7, United Kingdom), Beta (B.1.351, South Africa), Gamma (P.1, Brazil) and Delta (B.1.617.2, India). *J. Virus Erad.* **7**, 100054

44. Wu, L., Zhou, L., Mo, M., Liu, T., Wu, C., Gong, C., *et al.* (2022) SARS-CoV-2 Omicron RBD shows weaker binding affinity than the currently dominant Delta variant to human ACE2. *Signal. Transduct. Target. Ther.* **7**, 8

45. Gordon, D. E., Jang, G. M., Bouhaddou, M., Xu, J., Obernier, K., White, K. M., *et al.* (2020) A SARS-CoV-2 protein interaction map reveals targets for drug repurposing. *Nature* **583**, 459–468

46. Gentili, M., Kowal, J., Tkach, M., Satoh, T., Lahaye, X., Conrad, C., *et al.* (2015) Transmission of innate immune signaling by packaging of cGAMP in viral particles. *Science* **349**, 1232–1236

47. Schindelin, J., Arganda-Carreras, I., Frise, E., Kaynig, V., Longair, M., Pietzsch, T., *et al.* (2012) Fiji: an open-source platform for biological-image analysis. *Nat. Methods* **9**, 676–682